

# On the formation of voids in internal tin Nb<sub>3</sub>Sn superconductors

C. Scheuerlein<sup>a</sup>

*European Organization for Nuclear Research (CERN), CH-1211 Geneva, Switzerland*

M. Di Michiel

*European Synchrotron Radiation Facility (ESRF), 6 rue Jules Horowitz, F-38043 Grenoble, France*

A. Haibel

*Hahn-Meitner Institut Berlin (HMI), Glienicker Straße 100, D-14109 Berlin, Germany*

*13.2.2007*

*Accepted for publication in Applied Physics Letters*

The formation of voids during the reaction heat treatment of internal tin (IT) Nb<sub>3</sub>Sn strands degrades the physical superconductor properties. We describe three void growth mechanisms on the basis of combined synchrotron microtomography and x-ray diffraction results obtained during *in-situ* heating cycles. Initially void growth is driven by a reduction of void surface area. The main void volume increase is caused by density changes during formation of Cu<sub>3</sub>Sn in the strand. Long duration temperature ramps and isothermal holding steps neither reduce the void volume nor improve the chemical strand homogeneity prior to the superconducting A15 phase nucleation and growth.

---

<sup>a</sup> Author to whom correspondence should be addressed; electronic mail: Christian.Scheuerlein@cern.ch

The formation of voids during the reaction heat treatment (HT) of Nb<sub>3</sub>Sn superconductors has been an issue for several decades [1,2]. There is general agreement that it would be beneficial to avoid or at least control void growth, but the void formation mechanisms and possible remedies to limit void growth remain controversial. Previous studies of void growth in Nb<sub>3</sub>Sn strands have used destructive metallographic techniques. Since the void shape and distribution within Nb<sub>3</sub>Sn strands is strongly irregular, metallography results about void formation are erratic and can be strongly misleading. In contrast, a quantitative description of void volume, shape and distribution can be obtained using synchrotron micro-tomography [3]. Due to the short acquisition time of less than a minute per tomogram, tomography experiments during *in-situ* HT have recently become possible at the ID15A beamline at the European Synchrotron Radiation Facility (ESRF) [4]. In the present article we describe combined synchrotron micro-tomography and x-ray diffraction measurements during *in-situ* HT of an IT Nb<sub>3</sub>Sn strand. The void formation mechanisms are discussed by correlating the quantitative void growth results with the quantitative description of the phase transformations during the strand HT.

The sample analysed is a Nb<sub>3</sub>Sn strand of the IT design, which is described in detail in reference [5]. Within the diffusion barrier surrounding the 19 subelements of the strand, the Cu to Sn concentration ratio is approximately 82 wt.% Cu and 18 wt.% Sn. A metallographic cross section of the Nb<sub>3</sub>Sn strand after 1 h at 460 °C is presented in Figure 1. The black areas in the true colour images are voids. One can distinguish between relatively large voids in some of the diffusion centers and voids with sub- $\mu$ m dimensions, distributed around the filaments at the Cu-Sn intermetallic/ $\alpha$ -bronze interface.

Combined synchrotron micro-tomography and powder diffraction measurements were carried out at the ID15A high energy beamline of ESRF. Absorption micro-tomography was performed using a high intensity filtered white x-ray beam. The tomography set-up is described in detail in [4]. Powder diffraction measurements have been performed in transmission geometry, using an 88.005 keV monochromatic x-ray beam with a bandwidth of 0.1 keV. Debye-Scherrer diffraction patterns were acquired with a MAR 345 online image-plate detector. The experiment was optimised to obtain the best possible statistics. The resolution is not sufficient to distinguish between Nb and Ta (lattice constants 3.3066 Å and 3.3058 Å, respectively) and Nb-7.5wt.%Ta. Cu can not be distinguished from  $\alpha$ -bronze. *In-situ* heat treatments were performed in an inert gas atmosphere (He-H<sub>2</sub> mixture) in a dedicated furnace, which allows both tomographic and diffraction experiments. The accuracy of the sample temperature measurement is better than  $\pm 10$  °C over the entire temperature range.

A 3-D view of the voids present in the diffusion centers of the IT strand at different temperatures is shown in Figure 2. The tomograms have been acquired during *in-situ* HT with a ramp rate of 60 °C h<sup>-1</sup> with three additional isothermal holding steps for 2 h at 200 °C, 5 h at 340 °C and 2 h at 540 °C. The first voids are detected in the tomograms at 160 °C. The number of voids, the average void size and the average shape factor (calculated from the ratio void volume to void surface area) increase with increasing temperature. A maximum shape factor of 0.94 is obtained at 200 °C. Isothermal heating at 200 °C and Sn melting at 232 °C influence the void number, volume and shape only slightly. At about 280 °C an elongation of voids, whose diameter is approaching the Sn pool diameter of 50 µm, is observed. During the 5 h isothermal 340 °C HT the

agglomeration of globular voids to larger elongated voids continues. The number of voids detected decreases from 610 to 330, the average void volume increases from  $5.50 \times 10^3 \mu\text{m}^3$  to  $11.3 \times 10^3 \mu\text{m}^3$  and the average void shape factor decreases from 0.92 to 0.75. At 390 °C the maximum total void volume is obtained and several voids are extending over the entire sampled strand length of 1.3 mm. A drastic reduction of total void volume from  $5.7 \times 10^6$  to  $2.5 \times 10^6 \mu\text{m}^3$  occurs in the temperature interval 510 °C to 530 °C. During the isothermal 540 °C HT the number of small interfilament voids increases strongly (see Figure 3).

After each acquisition of a tomogram the sample was moved into the monochromatic x-ray beam for a powder diffraction measurement. A total of 110 diffractograms were acquired with the position sensitive detector during the *in-situ* strand HT. The 2-D diffraction patterns have been integrated into 1-D diffraction patterns and all are summarised in Figure 4. During the first stage of the HT up to 540 °C, which is often referred to as Cu-Sn mixing HT, five phase transformations are detectable. At first pure Sn and Cu are transformed into  $\text{Cu}_6\text{Sn}_5$  and  $\text{Cu}_3\text{Sn}$  by solid state diffusion. At around 230 °C the remaining Sn melts. Liquid Sn is present in the strand until 340 °C and vanishes entirely during the 340 °C isothermal holding step. The  $\text{Cu}_6\text{Sn}_5$  phase continues to grow until at 340 °C it reaches its maximum volume. The  $\text{Cu}_6\text{Sn}_5$  diffraction peaks decrease strongly in the temperature range 390 °C to 410 °C and vanish entirely between 410 °C and 420 °C. At 430 °C nearly all Sn in the strand is transformed into  $\text{Cu}_3\text{Sn}$ . The  $\text{Cu}_3\text{Sn}$  reflections vanish in the temperature region 500 °C to 540 °C and at the same time the  $\text{Cu}_{41}\text{Sn}_{11}$  peaks occur. During the isothermal 540 °C HT  $\text{Cu}_{41}\text{Sn}_{11}$  peak intensities decrease and  $\text{Cu}_{5,6}\text{Sn}$  peaks grow. The  $\text{Cu}_{5,6}\text{Sn}$  peaks grow until the formation of  $\text{Nb}_3\text{Sn}$

starts at about 580 °C and vanish entirely when the strand is completely reacted ( $\text{Nb}_3\text{Sn}$  growth results are not shown in Figure 4).

By correlating the quantitative tomography and diffraction results presented above, three different reasons for the formation of voids in IT  $\text{Nb}_3\text{Sn}$  superconductors can be described. The growth of the globular voids up to a temperature of about 200 °C is driven by a gain in free energy through a reduction of the total void surface area when smaller voids agglomerate to larger globular voids. It is assumed that voids are already introduced into the Sn during the production process used for the studied sample, but they are initially too small to be detected by the tomographic set-up. At 200 °C the maximum ratio of void volume to void surface area is obtained. At this temperature the total void volume ( $9.6 \times 10^{-5} \text{ mm}^3$ ) corresponds with 0.14 % of the entire strand volume, i.e. 2.5 % of the pure Sn volume. The densities reported for  $\text{Cu}_6\text{Sn}_5$ ,  $\text{Cu}_3\text{Sn}$  and  $\text{Cu}_{41}\text{Sn}_{11}$  exceed the densities of pure ( $\beta$ -) Sn and Cu in the corresponding stoichiometric quantities by 1 %, 4 % [6] and 3 %, respectively. Thus, the metal volume in the diffusion centers shrinks upon Cu-Sn intermetallic formation. Therefore, the void volume increases with  $\text{Cu}_3\text{Sn}$  content in the strand, and the maximum void volume is obtained when Sn is almost entirely transformed into  $\text{Cu}_3\text{Sn}$  (see Figure 5). Afterwards the void volume decreases strongly with increasing temperature until at 540 °C a minimum void volume is obtained. At the same time  $\text{Cu}_3\text{Sn}$  is entirely transformed into the lower density  $\alpha$ -bronze and  $\text{Cu}_{41}\text{Sn}_{11}$ . At 390 °C Sn is almost entirely transformed into  $\text{Cu}_3\text{Sn}$ , which occupies 22 vol.% of the sample. The maximum void volume ( $7.5 \times 10^{-3} \text{ mm}^3$ ) corresponds to 1.1 % of the sample volume. Thus, assuming a 4 % density increase upon  $\text{Cu}_3\text{Sn}$  formation, the void volume caused by density changes corresponds to 0.90 % of the strand volume.

During the solid state Cu-Sn interdiffusion there is a generation of vacancies due to differences of the diffusion coefficients of Cu in Sn and Sn in Cu. Under certain conditions the generation of vacancies can cause the nucleation and growth of voids, which are commonly referred to as Kirkendall voids [1,7]. The formation of the relatively small interfilament voids at the Cu-Sn intermetallic/ $\alpha$ -bronze interface is assumed to be caused by this effect. As compared to other samples, e.g. Sn solder joints and Sn coatings on Cu substrates [8], the void growth is observed at relatively high temperature, possibly because of stresses in the strand that prevent void growth at lower temperatures.

In summary, by combined *in-situ* tomography and diffraction measurements a quantitative description of the void growth and the phase transformations during the HT of an IT Nb<sub>3</sub>Sn strand has been obtained. Void growth in IT Nb<sub>3</sub>Sn strands is caused by three different mechanisms. The Sn in the non-heat treated strand contains voids that agglomerate during the first HT phase up to 200 °C. Subsequent heating causes void growth through density changes during intermetallic formation, in particular of Cu<sub>3</sub>Sn, and the formation of Kirkendall voids. Void growth is partly reversible when Cu-Sn intermetallics are transformed into the lower density  $\alpha$ -bronze. For the IT strand studied the influence of so-called isothermal “homogenisation” heat treatments on the microstructural and chemical strand homogeneity can be assessed from the combined tomography and diffraction results. Isothermal 340 °C heating causes the agglomeration of voids and, thus, reduces the microstructural strand homogeneity. During isothermal 540 °C heating the Cu<sub>5.6</sub>Sn phase grows and the interfilament void density is increased. Therefore, both isothermal holding steps are counterproductive in improving microstructural and chemical homogeneity.

**Acknowledgements**

The sample was kindly provided by Alstom-MSA. We are grateful to G. Arnau for EDS measurements and assistance in the phase analysis, and to R. Grupp for technical assistance at the tomography experiments.

We acknowledge the ESRF for beam time on ID15A and travel expenses.

C.S. acknowledges support from the European Community–Research Infrastructure Activity under the FP6 “Structuring the European Research Area” program (CARE, contract number RII3-CT-2003-506395).

## Figures and captions

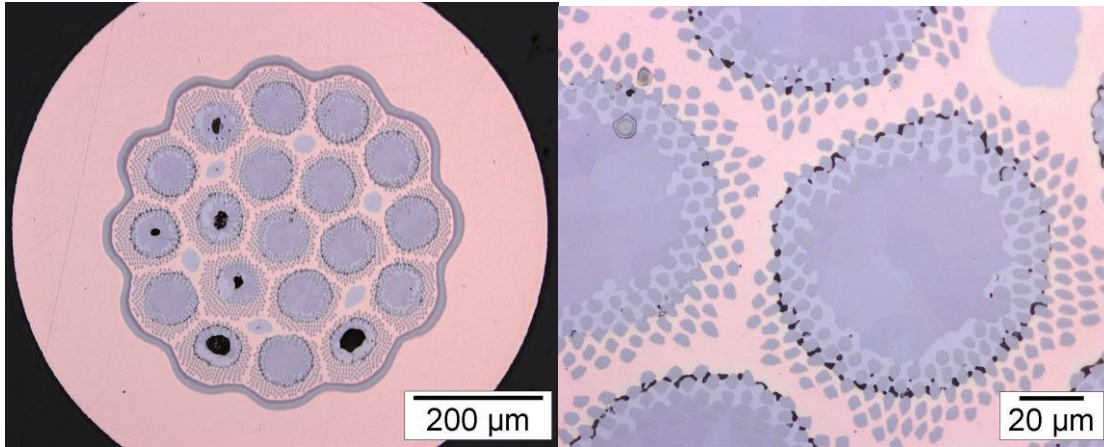


*Figure 1: IT Nb<sub>3</sub>Sn strand cross section after 460 °C ex-situ HT (ramp rate 6 °C h<sup>-1</sup>). The black areas in the true colour images are voids. After the 460 °C HT, most of Sn is in the form of Cu<sub>3</sub>Sn (dark grey), Cu<sub>41</sub>Sn<sub>11</sub> (bright grey) and some α-bronze.*



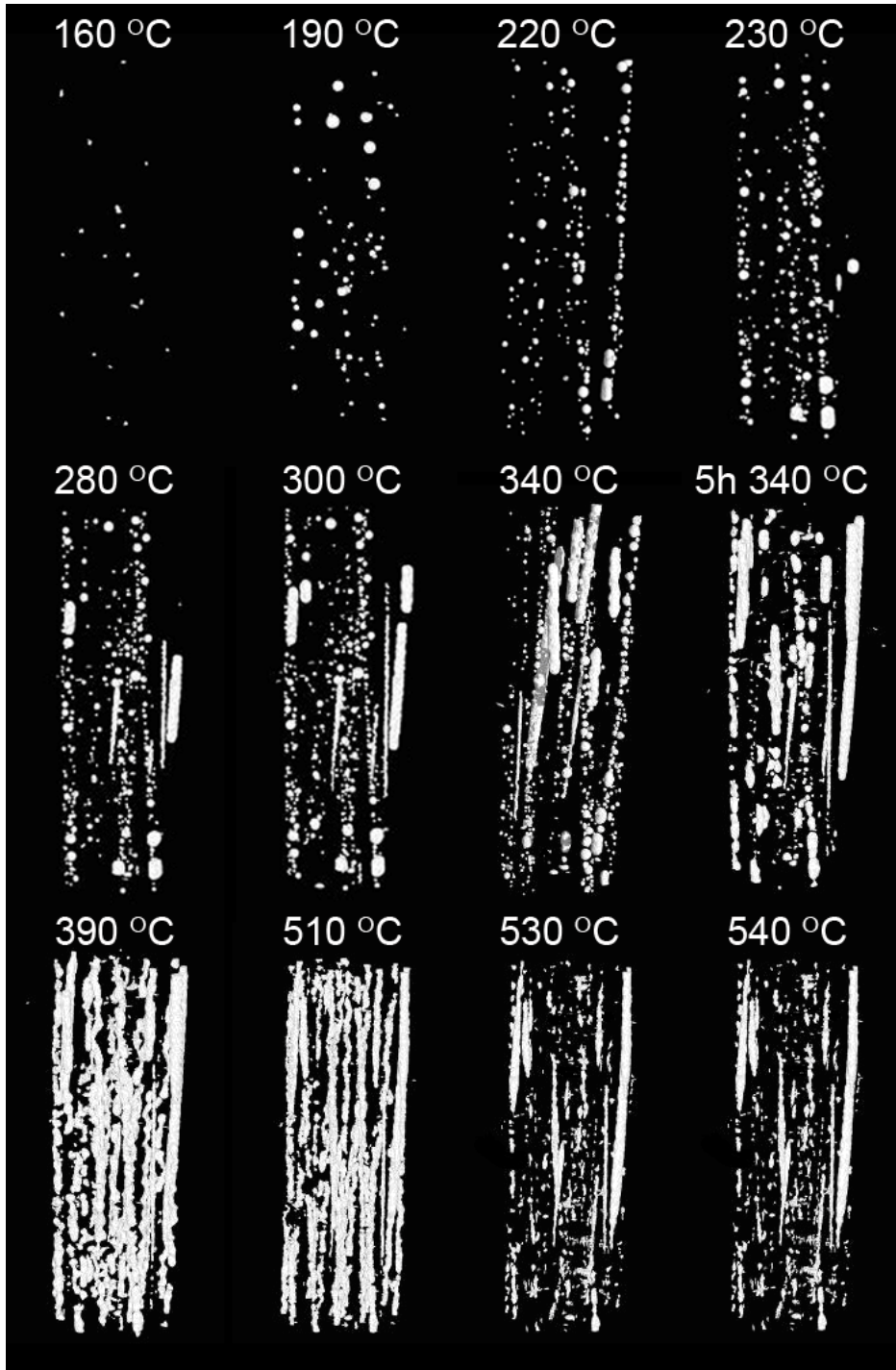


*Figure 2: 3-D view of the voids inside the IT strand at different HT temperatures. Binary images have been filtered in order to remove reconstruction artefacts.*

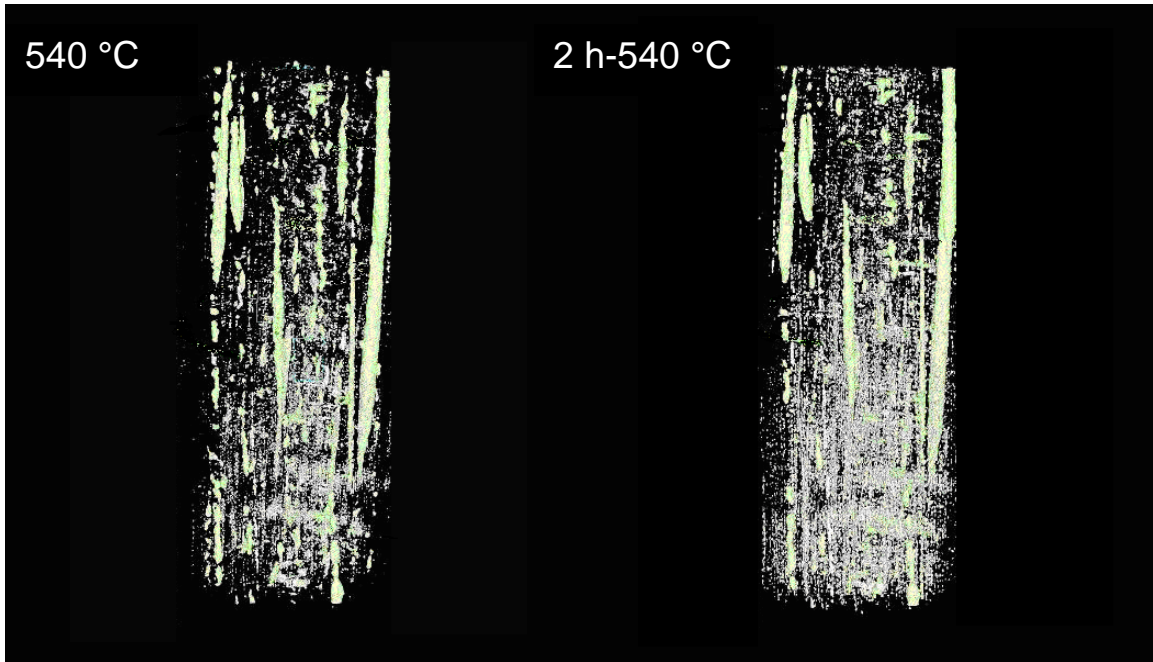


*Figure 3: Formation of interfilament voids during isothermal 540 °C HT. The volume of the interfilament voids with diameters in the order of 1  $\mu\text{m}$  can not be measured accurately and only the voids represented in yellow are taken into account in the determination of the void volume within the strand.*

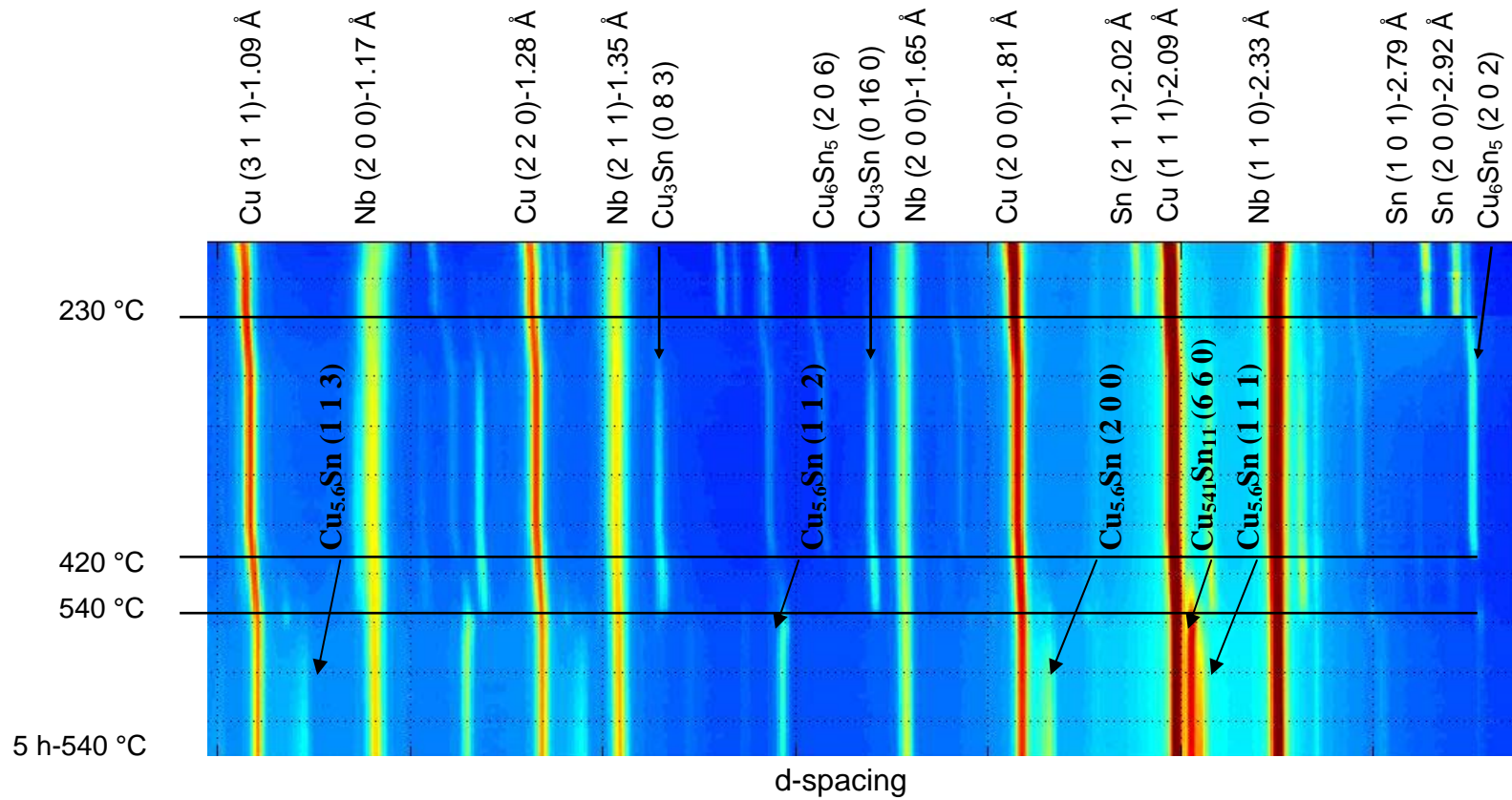


Figure 4: Variation of the diffraction patterns of the IT Nb<sub>3</sub>Sn during Cu-Sn mixing HT cycle between 120 °C and 540 °C (ramp rate 60 °C h<sup>-1</sup>, + isothermal 2 h-200 °C, 5 h-340 °C and 2 h-540 °C HT). Diffractograms have been acquired every 10 minutes.

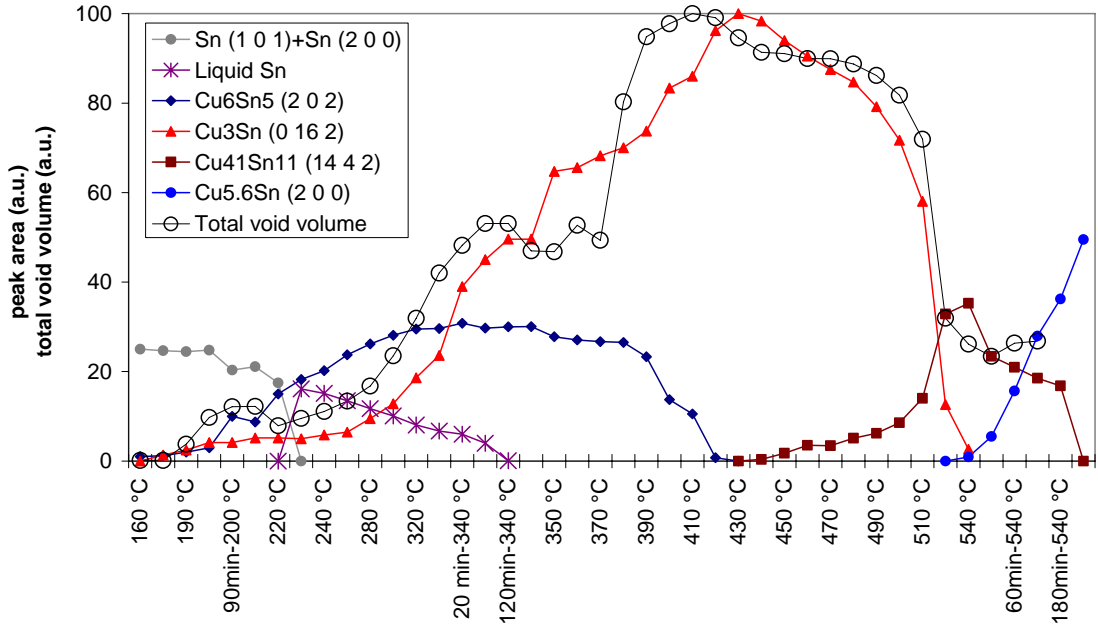


Figure 5: Peak areas of all Sn containing phases, apart from  $\alpha$ -bronze, that exist in the IT Nb<sub>3</sub>Sn strand during the reaction HT up to 540 °C. The peak areas have been scaled such that the values correspond with the intermetallics volume in the strand. For comparison the total void volume is also shown in the same plot. Void volume is clearly correlated with the Cu<sub>3</sub>Sn content in the strand.

## References

---

- 1 S. Cogan, D.S. Holmes, R.M. Rose, “On the elimination of Kirkendall voids in superconducting composites”, Appl. Phys. Lett. 35(7), pp. 557-559, (1979)
- 2 J.D. Verhoeven, A. Efron, E.D. Gibson, C.C. Cheng, “Void formation in Nb<sub>3</sub>Sn-Cu superconducting wire produced by the external tin process”, J. Appl. Phys., vol. 59(6), pp. 2105-2113, (1986)
- 3 A. Haibel, C. Scheuerlein, “Synchrotron tomography for the study of void formation in internal tin Nb<sub>3</sub>Sn superconductors”, accepted for publication in IEEE Trans. Appl. Supercon. 17(1), (2007)
- 4 M. Di Michiel, J.M. Merino, D. Fernandez-Carreiras, T. Buslaps, V. Honkimäki, P. Falus, T. Martins, O. Svensson, “Fast microtomography using high energy synchrotron tomography”, Rev. Sci. Instrum. 76, 043702, (2005)
- 5 M. Durante, P. Bredy, A. Devred, R. Otmani, M. Reyrier, T. Schild, F. Trillaud, „Development of a Nb<sub>3</sub>Sn multifilamentary wire for accelerator magnet applications“, *Physica C*, 354, pp. 449-453, (2001)
- 6 [http://www.metallurgy.nist.gov/mechanical\\_properties/solder\\_paper.html](http://www.metallurgy.nist.gov/mechanical_properties/solder_paper.html)
- 7 A. Paul, “The Kirkendall Effect in Solid State Diffusion”, PhD Thesis, Technische Universiteit Eindhoven, ISBN 90-386-2646-0, (2004)
- 8 C. Scheuerlein, Ph. Gasser, P. Jacob, D. Leroy, L. Oberli, M. Taborrelli, “The effect of CuSn intermetallics on the interstrand contact resistance in superconducting cables for the Large Hadron Collider”, J. Appl. Phys. 97(3), (2005)